Gorgan University of Agricultural Sciences and Natural Resources

Environmental Resources Research (ERR)

Print ISSN: 2783-4832
Online ISSN: 2783-4670

Determination of dew point temperature based on simultaneous multivariate models and vector time series considering heterogeneity in meteorological stations in eastern Iran

Abolfazl Akbarpour[1*], Vahid Khorramnezhad[2], Mohammad Nazeri Tahroudi[3]

[1] Professor, Department of Civil Engineering, Birjand University, Birjand, Iran
[2] M.Sc. student in Water Resources Managment, Department of Civil Engineering, Birjand University, Birjand, Iran
[3] Professor Assistant, Department of Water Engineering, Lorestan University, Khorramabad, Iran

Article Info

Article type:
Research Article

Article history:
Received: June 2024
Accepted: August 2024

Corresponding author:
Akbarpour@birjand.ac.ir

Keywords:
Modeling
Climate
Dew temperature
Time series
VAR model

Abstract

In this research, meteorological data from eleven stations were monitored to build a suitable model for predicting dew point values. Given the importance of dew point temperature in forecasting frosts, rainfall, and other meteorological applications, accurate prediction of this parameter is crucial. The stations included in the study are Bam, Birjand, Chabahar, Iranshahr, Kerman, Mashhad, Sabzevar, Tabas, Torbat Heydarieh, Zabul, and Zahedan, all located in dry climates. Initially, the correlation between various weather parameters and dew point was analyzed. Based on the highest correlation, three parameters—average, maximum, and minimum temperature—were selected as input variables for the model. CARMA and VAR models were used for analysis, and the stability of the residuals from both models was calculated. The series were then developed using the GARCH model. As a result, dew point modeling for the eleven meteorological stations was achieved with the CARMA-GARCH and VAR-GARCH models. Our findings show that the VAR-GARCH model outperformed the CARMA-GARCH model in both training and testing phases, making it the best model for this research. One key factor in the VAR-GARCH model's superior performance is its enhanced memory for processing time series data. The definitive result indicates that developing the residuals using the GARCH model improves the accuracy of both primary models by 6% to 30% in the testing phase.

Cite this article: Akbarpour, Abolfazl; Khorramnezhad, Vahid; Tahroudi Nazeri, Mohammad. 2024. Determination of dew point temperature based on simultaneous multivariate models and vector time series considering heterogeneity in meteorological stations in eastern Iran. *Environmental Resources Research*, 12(2), 229-256.

DOI: 10.22069/ijerr.2024.22535.1441
Publisher: Gorgan University of Agricultural Sciences and Natural Resources

Introduction

Dew point is a weather phenomenon that is known for its importance in the balance of water in dry and semi-dry areas. The dew point denotes the atmospheric temperature at which the air contains the maximum amount of moisture. The dew point and the ability to detect its presence have a broad scope of practical uses in various sciences, engineering, and meteorology. When the temperature reaches the dew point at a given pressure, the rate for water evaporation in liquid form and the rate for its vapor condensation become equal. As per the report by Aguirre-Gutiérrez and collaborators (2019), dew can contribute up to 2.10 of the yearly water influx and 6.33 of the complete dry season precipitation in a semi-dry continental prairies. (Aguirre-Gutiérrez et al., 2019). Maestre Valero et al. (2015) investigated the use of dew collectors as a novel approach to harnessing atmospheric moisture as a viable water resource (Maestre-Valero, Martin-Gorriz, & Martínez-Alvarez, 2015). Tomaszkiewicz and colleagues (2017) also demonstrated that dew harvesting can substantially enhance soil humidity levels, and can be used for afforestation and crop growth in dry and semi-arid environments (Tomaszkiewicz, Abou Najm, Zurayk, & El-Fadel, 2017), which demonstrates one of the important applications of dew. Zhang and colleagues (2015) and Zhang and colleagues (2019) emphasized the importance of dew as a water source, particularly due to its limited yet valuable contribution compared to traditional water sources, such as irrigation and rainfall (Yokoyama et al., 2021; Zhang et al., 2015; Zhang, Wang, Yue, & Wang, 2019).

Studies show that the Vector Autoregressive Generalized Conditional Heteroskedasticity (VAR-GARCH) model, if appropriately modified, can improve the accuracy of time series and ensure conditional heteroskedasticity stability. VAR-GARCH combination models are more accurate than vector models. The VAR model is a highly effective and adaptable framework for examining multivariate type of time series. The model represents a natural extension of the univariate autoregressive model for multivariate type of time series. The Vector Autoregressive (VAR) model was originally devised to capture and forecast complex fluctuations inherent in time series of financial and economic nature. The model frequently yields more accurate forecasts than those obtained from using simple and precise models for time series. VAR model forecasting capabilities are completely adaptable, as they can be conditioned on future paths of specified hypothetical variables. The model, beyond its descriptive and predictive capabilities, is employed for structural inference and policy evaluation as well. In the context of structural analysis, researchers impose explicit assumptions on the underlying data structure, and subsequently, the repercussions of unforeseen disturbances or innovations on designated variables are distilled into a concise summary. The effects are typically encapsulated by impulse response functions along with variance decomposition of forecast errors. The model concentrates on examining multivariate covariances that are constant over time. VAR models were introduced in economics by Sims (1980) (Sims, 1980). A comprehensive technical examination of VAR models is presented in the research of Luthekpohl (1991), while more recent reviews of VAR methodologies can be found in the research of Watson (1994), Lütkephol (2001), and Waggoner and Zha (1999) (LUTHEKPOHL, 1991; Lütkepohl, 2001; Waggoner & Zha, 1999; Watson, 1994).

The use of VAR models in financial data is discussed in the works Hamilton (1994), Campbell et al. (1997), Culbertson (1996), Mills (1999) and Tsay (2001) (Campbell, Lo, MacKinlay, & Whitelaw, 1998; Cuthbertson & Nitzsche, 2005; Hamilton, 2020; Mills & Markellos, 2008; Tsay, 2005). So far, many researches have been conducted in the field of modeling and forecasting weather parameters. Each of these studies has considered different perspectives. In studies conducted in different parts of the world, different methods have been used to study dew point temperature and different results have been

obtained (Aguirre-Gutiérrez et al., 2019; Baguskas, King, Fischer, D'Antonio, & Still, 2016; Lin et al., 2021; Tomaszkiewicz et al., 2017).

In the study by Shahidi, et al. (2020), the efficiency of a VAR model was investigated on a yearly basis utilizing evaporation dataset from the Iranian Salt Lake basin, spanning the statistical period of 1996 to 2015. The findings revealed that VAR and VAR-GARCH models both exhibited exceptional precision and correlation, with the model evaluation metrics corroborating this conclusion.The annual pan evaporation model leveraging the VAR-GARCH model demonstrated a notable enhancement of approximately 4% in its outcomes, surpassing the performance of the VAR model. Notwithstanding, the incorporation of a random intercept and the subsequent reduction in the model uncertainty, enabled the VAR-GARCH model to outperform the VAR model in estimating pan evaporation values, yielding more accurate results. However, owing to the computational intensity inherent in the GARCH model, the simpler VAR model can serve as a viable alternative (Shahidi, Ramezani, Nazeri-Tahroudi, & Mohammadi, 2020).

Ramezani et al. (2023) applied Copula-based and ARCH-based models to predict storms. This study employed VAR-GARCH, copula, and Copula-GARCH models to investigate the concurrent occurrence of storms in the Aras River basin, situated in northwestern Iran, across a 20-year span from 1998 to 2018. Based on the results, the VAR-GARCH model was more accurate than the Copula and Copula-GARCH models. The superior performance of the VAR-GARCH model in the process of simulations can be attributed to its ability to incorporate multiple lags and effectively model the variance attributed to the residual series. Notably, possessing real-time knowledge about the current storm enables the development of highly accurate predictions regarding the subsequent storm event. The application of this approach can be highly beneficial in effective flood management, as the resulting curves can be utilized to establish a reliable flood warning system for the basin (Ramezani, Nazeri Tahroudi, De Michele, & Mirabbasi, 2023).

In dry and semi-dry areas, non-precipitation water, which mainly includes fog, dew, and adsorption of water vapor, plays an important role in local ecosystems. While individual components of non-precipitation water have been the subject of separate investigations in the past, there has been a notable lack of research focused on the collective properties and interdependencies of these components. Notably, a scarcity of research has explored the formation and transformation of non-precipitation water components, and even fewer studies have investigated their impact on surface water balance and their influence on crop water demands in China. A novel approach for distinguishing the components of non-precipitation water was established by integrating lysimeter - based measurements and micrometeorological data collected from a station located in the summer monsoon transition zone in China. Daily time series of non-precipitation water components were presented. Among the research that has been done in hydrology studies using time series, we can mention the creation of a univariate and bivariate model, or different artificial intelligence models, etc. Also, in various studies conducted in different parts of the world, different methods have been used to study dew point temperature and different results have been obtained. However, so far no research has been conducted on simulating and forecasting dew point temperature using ARMA (Autoregressive Moving-Average) co-integration functions and vector models, as well as extended and hybrid models that consider anisotropy. This is because the effect of conditional variance has not been seen in multivariate simulations in various studies. The aim of this research is to simulate and predict dew point temperature in diverse climatic regions of Iran employing combined time series functions. Combined time series are one of the newest methods for multivariate analysis of hydrologic phenomena. Analyzing dew point temperature using multivariate and co-integrated time series

functions can lead to valuable information in hydrologic applications. The main innovation of this research is also the use of time series functions and conditional variance combinations to evaluate different input patterns to the simulation model. By employing these models, it is possible to provide the best prediction and simulation pattern of dew point temperature values in diverse climatic regions. This proposed approach will lead to the presentation of regional models for dew point prediction.

Accurate prediction of dew point temperature is crucial in a range of scientific disciplines, including hydrology, agriculture, and climatology. This is because many important parameters are involved in determining and calculating dew point temperature, including temperature (minimum, maximum, average), actual and saturation vapor pressures, relative humidity, and average monthly rainfall. Therefore, determining this parameter using a smaller number of parameters that can be easily measured at weather stations will be very efficient. The objective of the present study is to examine the accuracy of the simultaneous and vector time series model in simulating and predicting dew point temperature using different input patterns. Also, due to the stochastic nature of the series under study, investigating and modeling the remaining part of the series will increase the performance of the models under study, for which hybrid models of the Autoregressive Conditional Heteroscedasticity (ARCH) family were used.

Materials and Methods

Case study

The geographic scope of the study covers the provinces of South Khorasan, Razavi Khorasan, Kerman, and Sistan and Baluchestan. These provinces form the eastern part of Iran. In this study, dew point temperature values were modeled and predicted using weather data from 11 stations in eastern Iran. The stations studied in this research are shown in Figure (1) including the cities of Bam, Birjand, Chabahar, Iranshahr, Kerman, Mashhad, Sabzevar, Tabas, Torbat Heydariyeh, Zabol, and Zahedan.

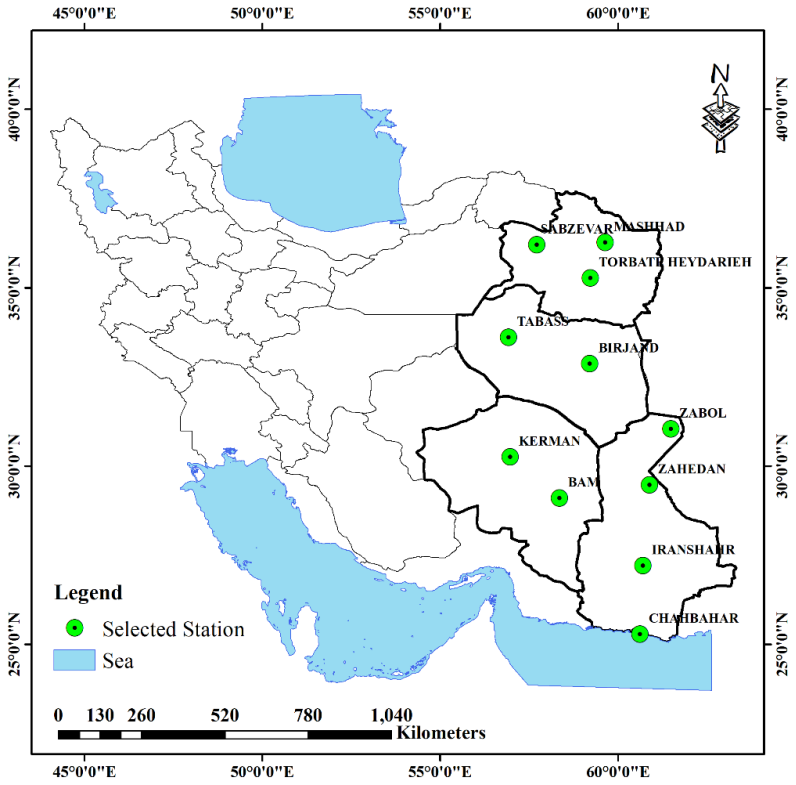

Figure 1. The geographic location details for the weather stations included in the study

Examining the statistical period of synoptic stations across the country revealed that, although the number of stations is considerable, few have long-term data suitable for studying climate change. The stations with the desired long-term statistical characteristics are listed, along with their specifications. While data from some stations date back to 1951, the statistical period of 1983–2021 was selected to include more stations and eliminate data inhomogeneity from the early years of operation.

Calculated Dew Point Values

At Bam station, the highest dew point values occur from July 10 to August 10, while the lowest dew point values are recorded from December 10 to January 10. Similarly, at the stations of Birjand, Chabahar, Iranshahr, Kerman, Mashhad, Sabzevar, Tabas, and Torbat Heydarieh, the highest dew point temperatures are observed in July (July 10 to August 10). In contrast, at Zabol and Zahedan stations, the highest dew point temperatures occur later, from August 11 to September 12.

The lowest dew point values at Bam, Birjand, Chabahar, Iranshahr, Kerman, Tabas, Torbat Heydarieh, Zabol, and Zahedan stations were recorded between November 10 and December 10. However, for Mashhad and Sabzevar stations, the lowest dew points occurred from January 10 to February 10. All data were calculated for the period 1983 to 2021. The minimum and maximum dew point values for all stations are presented in Table 1.

Table 1. Maximum and minimum dew point for the studied stations

Station	The average dew point temperature	The maximum dew point temperature
Bam	16	15.85
Birjand	16	17.76
Chabahar	26.4	36.95
Iranshahr	25.8	23.83
Kerman	15	17.03
Mashhad	15.7	27.69
Sabzevar	16.55	20.26
Tabas	20	15.88
Tprbat-e Heydarieh	20	22.10
Zabol	20	19.89
Zahedan	14.95	27.21

First, the correlation of various data (such as evaporation and transpiration-sunshine hours, wind speed at 10 meters height, average humidity, maximum and minimum temperature and average temperature) with the mentioned parameter (dew point) was measured and then 3 parameters (maximum temperature, minimum temperature, average temperature) were selected as model inputs with the highest correlation coefficient. In this research, we first used Continuous Autoregressive Moving Average (CARMA) and VAR methods. Then the random series or the remaining series was developed with the ARCH model and CARMA-GARCH and VAR-GARCH models were produced. Dew point modeling was performed using these 4 models and the results were finally analyzed and compared. The validation of the models and their efficiency were investigated in terms of RMSE and Nash-Sutcliffe criteria.

In this research, CARMA, VAR, and combined CARMA-GARCH and VAR-GARCH models are used for simulation and modeling of dew point temperature in various stations in eastern Iran. Also, maximum, minimum, and average temperature data are used on a monthly scale of the studied stations to form different inputs.

Simultaneous ARAMA model

The elements of the matrix for the autoregressive and moving average components are considered such that a multivariate model, separate and independent from the ARMA model, can be established. Therefore, instead of calculating the components of the model

simultaneously, they must be determined individually for each single-component ARMA site. This approach results in the identification of the best single-variable ARMA model for each site. If a full multivariate ARMA model is applied, rather than modeling a distinct temporal dependency structure for each site, a uniform temporal dependency structure can be assumed across all sites.

The CARMA(p,q) model for nn sites is calculated according to the following equation:

$$Y_t = \sum_{i=1}^{p} \phi_j Y_{t-j} + \varepsilon_t - \sum_{j=1}^{q} \theta_j \varepsilon_{t-j} \quad (1)$$

Y_t^k with a normal distribution and mean zero representing the different sites Y_t k=1,2,…,n، a n*1 column matrix of the observed series $\theta_1,\theta_2,...,\theta_q$ is the n*n matrix for the components of the moving average $\varphi_1,\varphi_2,...,\varphi_p$ model and the n*n diagonal matrix is the components of the autoregressive model. ε_t is also random data with normal distribution and zero mean, and variance-covariance g and a n*1 matrix of data.

$$\begin{bmatrix} Y_t^{(1)} \\ Y_t^{(2)} \\ \vdots \\ Y_t^{(n)} \end{bmatrix} = \begin{bmatrix} \varphi^{11} & \varphi^{12} & \cdots & \varphi^{1n} \\ \varphi^{21} & \varphi^{22} & \ldots & \varphi^{2n} \\ \vdots & \vdots & \ddots & \vdots \\ \varphi^{n1} & \varphi^{11} & \cdots & \varphi^{nn} \end{bmatrix} \begin{bmatrix} Y_{t-1}^{(1)} \\ Y_{t-1}^{(1)} \\ \vdots \\ Y_{t-1}^{(n)} \end{bmatrix} + \begin{bmatrix} \theta^{11} & \theta^{12} & \cdots & \theta^{1n} \\ \theta^{21} & \theta^{22} & \ldots & \theta^{2n} \\ \vdots & \vdots & \ddots & \vdots \\ \theta^{n1} & \theta^{n1} & \cdots & \theta^{nn} \end{bmatrix} \begin{bmatrix} \varepsilon_t^{(1)} \\ \varepsilon_t^{(2)} \\ \vdots \\ \varepsilon_t^{(n)} \end{bmatrix} \quad (2)$$

This model can preserve the zero lag cross-correlation in different sites and locations.

To calculate the components of the model, we consider N years of data for each site i with observational information, and $Y_t^{(i)}$ and i=1,2,3,…,n, the general model matrix Yt, is defined as follows:

$$Y_t = \mu + \sigma Z_t \quad (3)$$

where σ and μ are the variance and mean of Yt, respectively, and the standardization of the variables is obtained using the following equation:

$$Z_t^{(i)} = (y_t^{(i)} - \mu_t^{(i)}) / \sigma^{(i)}, i = 1,2,...,n \quad (4)$$

The components of the CARMA(p(i),q(i)) model are specified similar to the components of the ARMA model. The remaining time series of this model does not have a time variable, and this parameter has been completely removed, but it is dependent in space. This interdependence is calculated using the following equation:

$$\varepsilon_t^{\prime(i)} = \frac{\varepsilon_t^{(i)}}{\sigma_t^{(i)}} \quad (5)$$

$$\varepsilon_t' = B\xi_t \quad (6)$$

B is calculated as follows:

$$\hat{B}\hat{B}^T = \hat{M}_0 \quad (7)$$

where x is equal to the matrix of the autocorrelation function with zero delay, which is calculated from the following matrix:

$$\hat{M}_k = \begin{matrix} r_k^{11} & r_k^{12} & \cdots & r_k^{1n} \\ r_k^{21} & r_k^{22} & \cdots & r_k^{2n} \\ : & : & & : \\ r_k^{n1} & r_k^{n2} & \cdots & r_k^{nn} \end{matrix} \quad (8)$$

$$r_k^{ij} = \frac{\sum_{t=1}^{N-K} (\varepsilon_t^{(i)} - \bar{\varepsilon}_t^{(i)})(\varepsilon_{t+k}^{(i)} - \bar{\varepsilon}_{t+k}^{(i)})}{\sqrt{\sum_{t=1}^{N-K} (\varepsilon_t^{(i)} - \bar{\varepsilon}_t^{(i)})^2 \cdot \sum_{t=1}^{N-K} (\varepsilon_{t+k}^{(i)} - \bar{\varepsilon}_{t+k}^{(i)})^2}} \quad (9)$$

where $\bar{\varepsilon}_{t+k}^{(i)}$ is the N-K mean of data j and $\bar{\varepsilon}_t^{(i)}$ is the N-K mean of data i. Finally, the matrix of the components of the CARMA(p,q) model is calculated by the method (Matalas, 1967):

$$\hat{A}_1 = \hat{M}_1 \hat{M}_0^{-1} \quad (10)$$

Vector Autoregressive (VAR) Model

The vector autocorrelation model is a statistical technique employed to establish a linear relationship among several variables. It employs a self-correlated integrated model, where all the variations are incorporated simultaneously. Each value in the VAR model is explained by an equation

that takes into account its own variation as well as the variations from other models, along with an error term. Understanding the forces at play in VAR modeling requires a significant amount of knowledge, as there are no pre-existing structural models with the necessary equations. Despite this complexity, the VAR model is widely used in econometrics and efficiency estimations, and it has been economically validated. However, there have been no studies conducted on this subject in our country. If $Y_t = (y_{1t}, y_{2t}, \ldots, y_{nt})^{/}$ indicates the vector of time series variables (n×1), the VAR(p) model with a p-year basis can be expressed as follows:

$$\varepsilon_t = \sigma_t z_t \quad and \quad \sigma_t^2 = a_0 + \sum_{i=1}^{m} b_i \varepsilon_{t-i}^2 \qquad (11)$$

The coefficient Πi represents the (n × n) element of the matrix, while εt represents the (n × 1) matrix consisting of independent white noise values with zero mean and a constant covariance matrix Σ. To illustrate, the equation of the VAR model with two variables can be expressed as follows:

$$\begin{pmatrix} y_{1t} \\ y_{2t} \end{pmatrix} = \begin{pmatrix} c_1 \\ c_2 \end{pmatrix} + \begin{pmatrix} \pi_{11}^1 & \pi_{12}^1 \\ \pi_{21}^1 & \pi_{22}^1 \end{pmatrix} \begin{pmatrix} y_{1t-1} \\ y_{2t-1} \end{pmatrix} + \begin{pmatrix} \pi_{11}^2 & \pi_{12}^2 \\ \pi_{21}^2 & \pi_{22}^2 \end{pmatrix} \begin{pmatrix} y_{1t-2} \\ y_{2t-2} \end{pmatrix} + \begin{pmatrix} \varepsilon_{1t} \\ \varepsilon_{2t} \end{pmatrix} \qquad (12)$$

$$\begin{aligned} y_{1t} &= c_1 + \pi_{11}^1 y_{1t-1} + \pi_{12}^1 y_{2t-1} + \pi_{11}^2 y_{1t-2} + \pi_{12}^2 y_{2t-2} + \varepsilon_{1t} \\ y_{2t} &= c_2 + \pi_{21}^1 y_{1t-1} + \pi_{22}^1 y_{2t-1} + \pi_{21}^2 y_{1t-1} + \pi_{22}^2 y_{2t-1} + \varepsilon_{2t} \end{aligned} \qquad (13)$$

The value $cov(\varepsilon_{1t}, \varepsilon_{2t}) = \sigma_{12}$ is zero when t equals s, and for all other values of t, it is different from zero. It is important to highlight that each individual equation represents a regression of the residuals y1t and y2t, and therefore, the VAR (p) model can be seen as an indirect regression model with residual variables and deterministic terms, similar to usual regressions. From an end-user's standpoint, the VAR (p) model is expressed as relation (14):

$$\Pi(L)Y = c + \varepsilon_t \qquad (14)$$

where $\Pi(L) = I_n - \Pi_1 L - \ldots - \Pi_1 L^p$. If the determinant $(I_n - \Pi_1 z - \ldots - \Pi_p z^p)$ equals zero, the VAR(p) model will become stationary. In the case where the eigenvalues of the composite matrix have a modulus less than one, outside the complex unit loop (with a modulus greater than one), or equivalently, if the eigenvalues of the composite matrix have a modulus smaller than unity, it is presumed that the operation started at infinity in the distant past. Consequently, it is a stable VAR(p) process with constant mean variance and covariance. If Y_t has a constant covariance in relation 1, then the mean can be expressed in the form of equation 16.

$$F = \begin{pmatrix} \Pi_1 & \Pi_2 & \cdots & \Pi_n \\ I_n & 0 & \cdots & 0 \\ 0 & . & 0 & : \\ 0 & 0 & I_n & 0 \end{pmatrix} \qquad (15)$$

$$\mu = (I_n - \Pi_1 - \ldots - \Pi_p)^{-1} c \qquad (16)$$

Following the normalized mean obtained from the VAR(p) model:

$$Y_t - \mu = \Pi_1 (Y_{t-1} - \mu) + \Pi_2 (Y_{t-2} - \mu) + \ldots + \Pi_p (Y_{t-p} - \mu) + \varepsilon_t \qquad (17)$$

The fundamental VAR(p) model might have certain limitations in capturing the underlying patterns and properties inherent in the data. Specifically, additional deterministic conditions like a linear time trend or seasonal variables could be used to accurately represent the data. Moreover, random variables might be necessary as well. The overall structure of the VAR(p) model with deterministic components and external variables is outlined as follows:

$$Y_t = \Pi_1 Y_{t-1} + \Pi_2 Y_{t-2} + \ldots + \Pi_p Y_{t-p} + \Phi D_t + G X_t + \varepsilon_t \qquad (18)$$

where, $D_t$is equal to the matrix (lx1) of deterministic components, X_t is equal to the matrix (mx1) of external variables, Φ and G are the model parameters matrix as well.

Conditional vector autocorrelation model considering anisotropy (ARCH Model)

ARCH models were first introduced by Engle (1982) for economic models and are the first models with a systematic procedure

for modeling volatility (Engle, 1982). ARCH models work in two ways: (a) the mean-adjusted return on investment is separate but dependent, and (b) the model is dependent and can be represented by a second-order function of the previous data. In general, the ARCH model is considered as follows:

where σ_t^2 represents the conditional variance, ε_t denotes the residual or error term of the model, which is characterized by a zero mean and a unit variance, a_0≥0, b_i≥0 are the model parameters , m is the model order and Zt represents the time series data corresponding to the parameter of interest. For a deeper understanding of the ARCH model, the architecture of the ARCH(1) model.

$$\alpha_t = \sigma_t \varepsilon_t \ , \ \sigma_t^2 = \alpha_0 + \alpha_1 \alpha_{t-1}^2 \quad (19)$$

where $\alpha_0 > 0$ and $\alpha_1 \geq 0$. Initially, it is essential to assume that the conditional mean denoted by α_t is equal to zero. This is because:

$$E(\alpha_t) = E[E(\alpha_t|F_{t-1})] = E[\sigma_t E(\varepsilon_t)] \quad (20)$$

The conditional variance is calculated as below:

$$\begin{aligned} Var(\alpha_t) &= E(\alpha_t^2) \\ &= E[E(\alpha_t^2|F_{t-1})] \\ &= E[\alpha_0 + \alpha_1 a_{t-1}^2] \\ &= \alpha_0 + \alpha_1 E(\alpha_{t-1}^2) \end{aligned} \quad (21)$$

where considering $E(\alpha_t) = 0$, $Var(\alpha_t) = E(\alpha_{t-1}) = E(\alpha_{t-1}^2)$, α_t is a fixed and static process. Thereby, we have:

$$Var(\alpha_t) = \alpha_0 + \alpha_1 VAR(\alpha_t) \quad (22)$$

$$Var(\alpha_t) = \frac{\alpha_0}{(1-(\alpha_0))} \quad (23)$$

Since variance α_t must be greater than zero, as a result, α_1 can be at most one. In some cases, there must be values greater than (α_t), Therefore, α_1 must generate a surplus of torque. For instance, when examining the behavior in sequences, the fourth moment (α_t) should be limited. Considering normality ε_t in the equation, we have:

$$\begin{aligned} E(\alpha_t^4|F_{t-1}) &= 3[E(\alpha_t^2|F_{t-1})]^2 \\ &= 3(\alpha_0 + \alpha_1 \alpha_{t-1}^2)^2 \end{aligned} \quad (24)$$

$$\begin{aligned} E(\alpha_t^4) &= E[E(\alpha_t^4|F_{t-1})] \\ &= 3E(\alpha_0 + \alpha_1 \alpha_{t-1}^2)^2 \\ &= 3E(\alpha_0^2 + 2\alpha_0 \alpha_1 \alpha_{t-1}^2 + \alpha_1^2 \alpha_{t-1}^4) \end{aligned} \quad (25)$$

If α_t is treated as the fourth constant term and $\mathrm{m}_4 = \mathrm{E}(\alpha_t^4)$, then:

$$m_4 = 3E(\alpha_0^2 + 2\alpha_0 \alpha_1 Var(\alpha_t) + \alpha_1^2 m_4) = 3\alpha_0^2 \left(1 + 2\frac{\alpha_1}{1-\alpha_1}\right) + 3\alpha_1^2 m_4 \quad (26)$$

Finally,

$$m_4 = \frac{3\alpha_0^2(1+\alpha_1)}{(1-\alpha_1)(1-3\alpha_1^2)} \quad (27)$$

Model evaluation criteria

By using two factors, the root mean square error (RMSE) and the Nash-Sutcliffe coefficient (NSE), it is possible to find the best model based on the minimum RMSE (28) and the maximum NSE (29):

$$RMSE = \left[\frac{\sum_{i=1}^{n}(\hat{Q}_i - Q_i)^2}{N}\right]^{0.5} \quad (28)$$

$$CE = 1 - \frac{\sum_{i=1}^{T}(Q_i - Q_i')^2}{\sum_{i=1}^{T}(Q_i - \overline{Q}_\iota)^2} \quad (29)$$

In the above equations, $\overline{Q}$، Q'، Q_i are the mean dew point, the calculated dew point, the observed dew point, respectively with n denoting the total number of data points. In order to combine linear models with a group of nonlinear models, in the first step, the information and data will be calculated using linear models, and then the remaining series of calculations and models will be fitted with a nonlinear model [7,8,9].

Results and Discussion

According to Table 2, the parameters that have the highest correlation coefficients with the dew point at all stations studied are temperature in terms of average temperature, maximum temperature, and minimum temperature. These three parameters are used as inputs for the models. As mentioned earlier, the number

of inputs for each of the four models is three. The next parameters that have the highest correlation with the dew point are potential evapotranspiration and sunshine hours per day.

Table 2. Correlation of data with dew temperature

Station	Studied parameters						
	Evaporation and transpiration potential	sunny hours	Wind speed at a height of 10 meters	Average relative humidity	Average temperature	Minimum temperature	Maximum temperature
Bam	0.62	0.53	0.18	-0.37	0.78	0.72	0.74
Zabol	0.64	0.62	0.59	-0.38	0.77	0.70	0.74
Torbat-e Heydarieh	0.52	0.50	0.42	-0.33	0.78	0.62	0.69
Tabas	0.50	0.47	0.24	-0.26	0.6	0.55	0.57
Sabzevar	0.59	0.52	0.46	-0.42	0.78	0.62	0.63
Mashhad	0.57	0.50	0.46	-0.37	0.83	0.61	0.65
Kerman	0.50	0.41	0.14	-0.24	0.74	0.52	0.61
Iranshahr	0.60	0.16	0.22	-0.08	0.76	0.75	0.78
Chabahar	0.68	0.63	0.20	-0.05	0.97	0.377	0.93
Birjand	0.48	0.42	0.36	-0.21	0.69	0.57	0.64
Zahedan	0.54	0.32	-0.05	-0.17	0.67	0.55	0.62

The De Martonne Index for Climate Classification of the Studied Stations

The De Martonne approach was employed to investigate and classify the climatic conditions in the regions and stations under examination. The outcomes of the climate analysis of different stations are shown in Table 3.

Table 3. The De Martonne index for the studied stations

Station	Average annual rainfall	Average temperature	Climate	De Martonne index
Bam	68	16	Dry	2.615
Birjand	168.5	16	Dry	6.48
Chabahar	110	26.4	Dry	3.02
Iranshahr	105	25.8	Dry	2.93
Kerman	142	15	Dry	5.68
Mashhad	250	15.7	Dry	9.72
Sabzevar	169	16.55	Dry	6.36
Tabas	80	20	Dry	2.66
Torbat-e Heydarieh	250	20	Dry	8.33
Zabol	61	20	Dry	2.03
Zahedan	89	14.95	Dry	3.56

Modeling and calculation method

First, we modeled the data using two models, CARMA and VAR. Then, the random coefficient (remaining series) extracted from the two models was developed using the GARCH model, resulting in the production of two models, CARMA-GARCH and VAR-GARCH. To train these models, 80% of the data was used at each station and the model was trained. Then, the models were tested with the remaining 20% of the data. In other words, using the output of the models and the values predicted by them, the obtained values are compared with the remaining 20% of the data to compare the models performance at each station. To assess the models performance and validate them, two parameters were used: the RMSE and NSE. The data is monthly from 1983 to 2021 (457 months). The data of 367 months, representing 80% of the data, was entered into the models for the testing phase, and then the output of the model was compared with the remaining 90 months of data.

Results of modeling dew point values in the studied stations based on the CARMA model

Initially, 80% of the data was utilized to

train the model. Subsequently, the model underwent training, and its outputs were generated during the testing phase spanning from 2013 to 2021, based on the information provided in Table (4). These outputs were then adjusted to match the actual values. Evaluating the performance of the model, quantified by the RMSE and NSE, was conducted for both the training and testing phases of the CARMA model across 11 study stations. The detailed results can be found in Table (4).

Table 4. Dew point modeling results in training and testing phase based on CARMA model

Station	RMSE		Nash-Sutcliffe Coefficient	
	Training	Testing	Training	Testing
Bam	3.05	2.67	0.53	0.58
Birjand	4.10	1.54	0.26	0.85
Chabahar	3.16	3.42	0.89	0.90
Iranshahr	3.38	1.94	0.64	0.90
Kerman	4.16	1.81	0.39	0.73
Mashhad	4.90	3.38	0.46	0.37
Sabzevar	3.37	2.13	0.51	0.68
Tabas	2.79	1.61	0.44	0.65
Torbat-e Heydarieh	4.19	2.64	0.47	0.57
Zabol	3.00	2.28	0.60	0.66
Zahedan	3.75	1.88	0.44	0.73

Determine the appropriate number of ACF delays

The VAR model analyzes various time lags in order to determine the optimal lag for incorporating data into the model. This feature of the VAR model enhances the model in comparison to linear models that do not take lag into account. Based on the findings, a lag of 3 was identified as the most suitable delay for inputting data from 10 stations into the model, while for the Tabas station, a delay of 2 was deemed appropriate for introducing data into the model.

The outcomes of modeling and simulation of dew point values at the investigated stations based on VAR model

Table (5) presents the comparison between the actual dew temperature data and the model output values during the training and testing phases for 11 study stations. The model was trained using 80% of the data up until the month of 367, while the remaining data from the month of 367 to 457 was used for testing the model's performance against the real data. The VAR model for the 11 study stations is detailed in Table (5).

Table 5. Dew point modeling results in training and testing phase based on VAR model

Station	RMSE		Nash-Sutcliffe Coefficient	
	Training	Testing	Training	Testing
Bam	1.69	1.30	0.86	0.90
Birjand	2.02	1.68	0.82	0.82
Chabahar	1.67	3.47	0.97	0.89
Iranshahr	1.74	2.10	0.91	0.88
Kerman	2.02	1.70	0.86	0.76
Mashhad	2.29	3.06	0.88	0.48
Sabzevar	1.82	1.99	0.86	0.72
Tabas	1.54	1.70	0.83	0.61
Torbat-e Heydarieh	2.07	2.62	0.87	0.57
Zabol	1.51	2.34	0.90	0.64
Zahedan	2.02	1.68	0.83	0.79

Comparing the CARMA and VAR models

In the training phase for the VAR model at Bam station, the root mean square error value is 1.69 degrees Celsius. On the other hand, the training phase for the CARMA model at the same station has an error value of 3.05 degrees Celsius. The efficiency coefficient for the VAR model in the training phase is 0.86, while for the CARMA model it is 0.53. Generally, the

VAR model shows lower error and higher efficiency coefficient during the training phase. Moving on to the testing phase, the error value for the VAR model is 1.30 degrees Celsius, with a Nash-Sutcliffe coefficient of 0.90. In contrast, the CARMA model has an error value of 2.67 degrees Celsius and a Nash-Sutcliffe coefficient of 0.58 in the testing phase. Overall, the VAR model outperforms the CARMA model at Bam station, demonstrating 55% better efficiency and 51% less error in the testing phase.

In all 11 stations that were investigated, the VAR model has consistently demonstrated superior performance in terms of error coefficient and model efficiency coefficient during the training phase, when compared to the CARMA model. However, during the testing phase, the CARMA model outperformed the VAR model only in the Iranshahr station. Specifically, the Nash-Sutcliffe coefficient for the CARMA model in the testing phase was 0.90, whereas for the VAR model it was 0.88. Additionally, the CARMA model exhibited a 7.6% lower error rate compared to the VAR model.

Studying the stability of the residual series for the VAR model

Prior to fitting the GARCH model, an examination was conducted on the residual or random series structural stability using ordinary least square (OLS) regression and Cumulative Sum (Cusum) tests. The Cusum test employs a particular approach from a broader statistical framework to calculate the empirical volatility process. The outcomes of this particular test were further validated based on the shape and confidence intervals. Notably, the OLS-based CUSUM process remained within the confidence intervals (CIs) (red lines) at all stations, indicating no evidence of structural changes. Consequently, the residual series exhibits the necessary stability to be incorporated into the GARCH model and, subsequently, analyze the common frequency of the residual series in CARMA and VAR models in the next step.

Modeling results of dew point values in the studied stations based on CARMA-GARCH model

Table (6) presents the comparison between the actual dew temperature data and the model's output values during the training and testing phases for 11 study stations. The model was trained using 80% of the data up until the month of 367, while the remaining data from the month of 367 to 457 was used for testing the model's performance against the real data.

Table 6. Dew point modeling results in training and testing phase based on CARMA-GARCH 6 model

Station	RMSE		Nash-Sutcliffe Coefficient	
	Training	Testing	Training	Testing
Bam	2.87	2.53	0.58	0.63
Birjand	3.90	1.39	0.33	0.88
Chabahar	2.96	3.05	0.9	0.92
Iranshahr	3.23	1.71	0.71	0.92
Kerman	4.08	1.4	0.41	0.84
Mashhad	4.69	3.15	0.51	0.45
Sabzevar	3.27	1.67	0.54	0.80
Tabas	2.61	1.37	0.51	0.75
Torbat-e Heydarieh	4.15	2.48	0.48	0.62
Zabol	2.80	1.98	0.66	0.74
Zahedan	3.62	1.49	0.46	0.83

Results of modeling the dew point values in the studied stations based on VAR-GARCH model

Table (7) displays the comparison between the actual dew temperature data and the model's output values during the training and testing phases for 11 study stations. The model was trained using 80% of the data up until the month of 367, while the remaining data from the month of 367 to 457 was used for testing the model's performance against the real data.

Table 7. Dew point modeling results in training and testing phase based on VAR-GARCH model

Station	RMSE		Nash-Sutcliffe Coefficient	
	Training	Testing	Training	Testing
Bam	1.32	0.99	0.94	0.91
Birjand	1.75	1.37	0.87	0.88
Chabahar	1.27	2.33	0.98	0.9
Iranshahr	1.42	1.74	0.94	0.92
Kerman	1.86	1.4	0.88	0.84
Mashhad	2.08	3.08	0.9	0.47
Sabzevar	1.55	1.69	0.9	0.79
Tabas	1.19	1.37	0.9	0.75
Torbat-e Heydarieh	1.89	2.48	0.89	0.62
Zabol	1.22	3.02	0.93	0.73
Zahedan	1.74	1.53	0.88	0.82

Comparison of CARMA-GARCH and VAR-GARCH models

During the training phase, the VAR-GARCH model exhibited superior performance relative to the CARMA-GARCH model across all investigated stations. In the subsequent testing phase, the VAR-GARCH model emerged as the top-performing model in 7 out of the 11 stations, namely Bam, Birjand, Iranshahr, Kerman, Tabas, Torbat Heydarieh, and Mashhad. Conversely, the CARMA-GARCH model demonstrated superior performance relative to the VAR-GARCH model in 4 stations, namely Sabzevar, Zabol, and Chabahar.

Examining different models and presenting the best model

The dew point values in the studied stations (Bam, Birjand, Chabahar, Iranshahr, Kerman, Mashhad, Sabzevar, Tabas, Tarbiat Heydarieh, Zabul, Zahedan) were estimated using four different models. These models utilized simultaneous models and time series vectorization with Anisotropy. In the training phase, verification and validation of different patterns were conducted in other stations. Based on the obtained figures, it can be observed that the closer the black points are to the black line, the higher the correlation of the data. The red lines denote the 95% CI. If there are more data points or black points outside the range, it indicates a higher error in the model. When comparing the four models, it was found that the VAR and VAR-GARCH models exhibited higher correlation and also accuracy during the training phase compared to the other two models. Furthermore, the CARMA-GARCH and VAR-GARCH models demonstrated the best correlation and accuracy during the testing phase, which is crucial. The efficiency and accuracy of the models were fully evaluated in terms of RMSE and model efficiency coefficient (NSE) during both the training and testing phases. Figure (2) displays the estimated dew point values for the Bam station, while the remaining stations are provided in the appendix. Figure.A.1 for Birjand Station, Figure.A.2 for Chabehar Station, Figure.A.3 for Iranshahr Staion, Figure.A.4 for Kerman Station, Figure.A.5 for Mashad Station, Figure.A.6 Sabzevar Station, Figure.A.7 Tabas Station, Figure.A.8 Torbat Heidarie Station, Figure.A.9 Zabol Station and Figure.A.10 for Zahedan Station displays the estimated dew point values based on all presented models in this study.

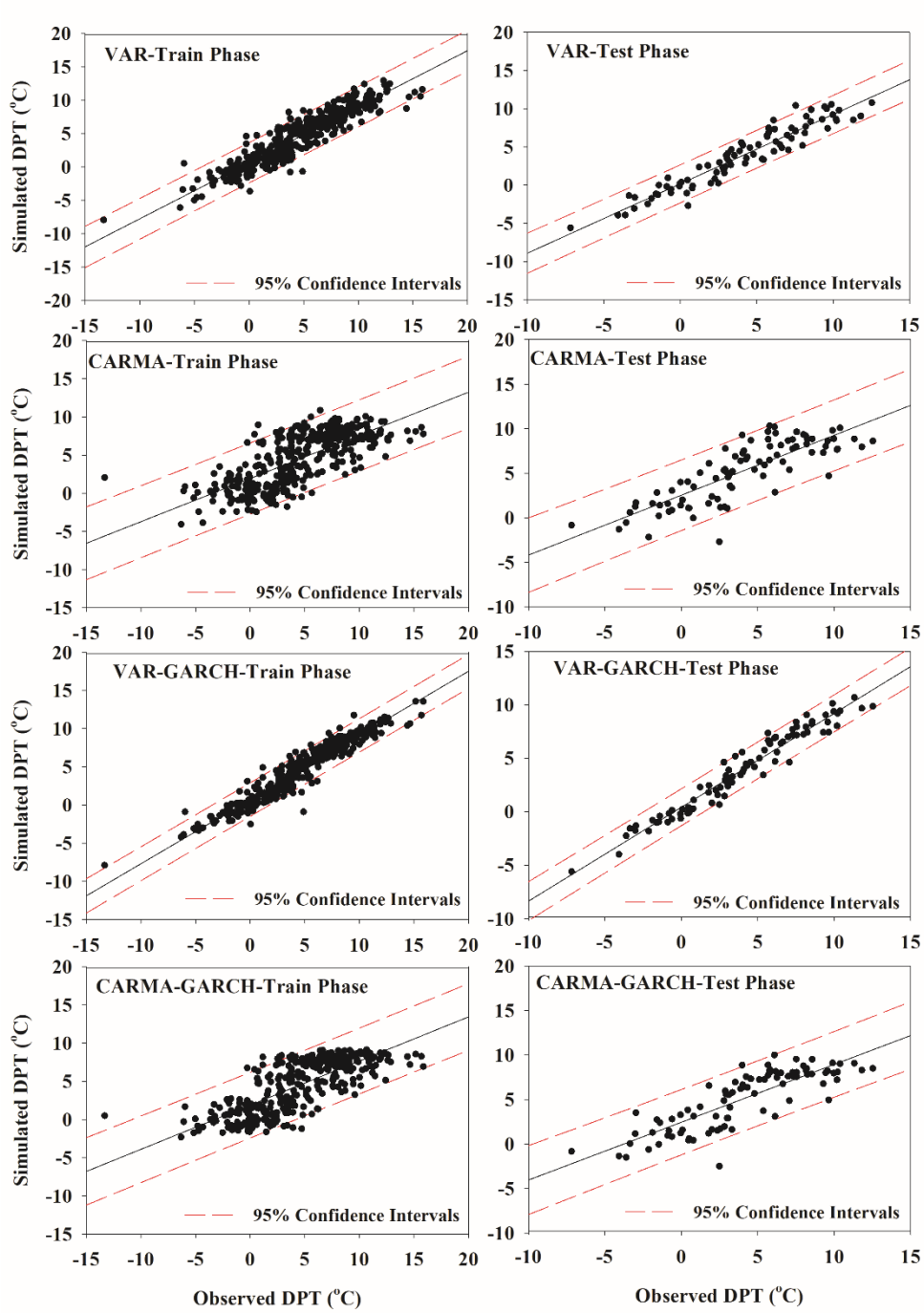

Figure 2. The outcomes of assessing and measuring the accuracy of estimated dew point values in Bam station

Nash-Sutcliffe criterion (in training and testing phase)

The Nash-Sutcliffe criterion is depicted in Figure (3) during the training phase for comparison, while Figure (4) illustrates it during the testing phase. Based on Figure (2), it is evident that the VAR-GARCH model outperforms all other models in the training phase, ranking second only to the VAR model. Furthermore, in the testing phase, both the VAR-GARCH and CARMA-GARCH models exhibit comparable performance, as indicated by Figure (3). However, the CARMA-GARCH model displays a higher error rate, whereas the VAR-GARCH model demonstrates consistent performance across different stations.

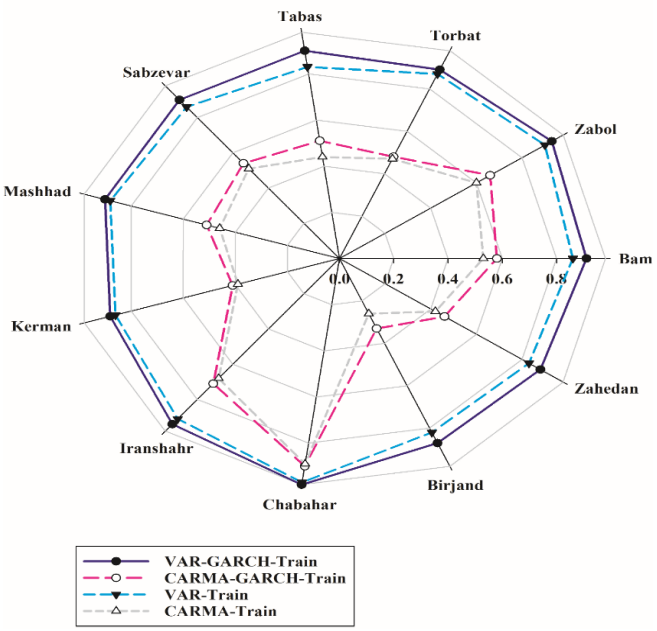

Figure 3. Model efficiency criterion (Nash-Sutcliffe) of stations in the training phase

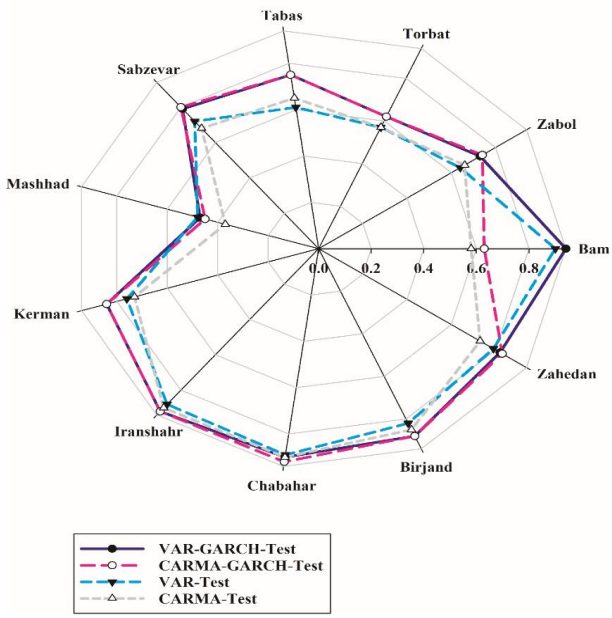

Figure 4. Model efficiency criterion (Nash-Sutcliffe) of stations in the testing phase

Root mean square error (in training and testing phase)

The training phase results for the root mean square error criteria can be observed in Figure (5), while the testing phase results are depicted in Figure (6). Figure (5) indicates that the VAR-GARCH model outperforms all other models in the training phase, providing the best performance. The VAR model, on the other hand, exhibits the best performance in the training phase and ranks as the second-best model. In the testing phase, both the VAR-GARCH and CARMA-GARCH models demonstrate similar performance, as shown in Figure (6). However, based on the output of the Bam station during the testing phase, the CARMA-GARCH model exhibits a higher difference in error magnitude relative to the VAR-GARCH model. Consequently, we can anticipate a more reliable output from the VAR-GARCH model.

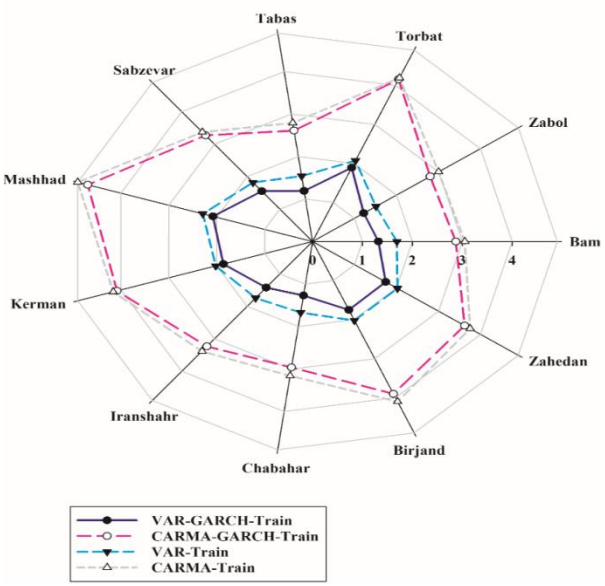

Figure 5. Model error measure (RMSE) of the stations in the training phase

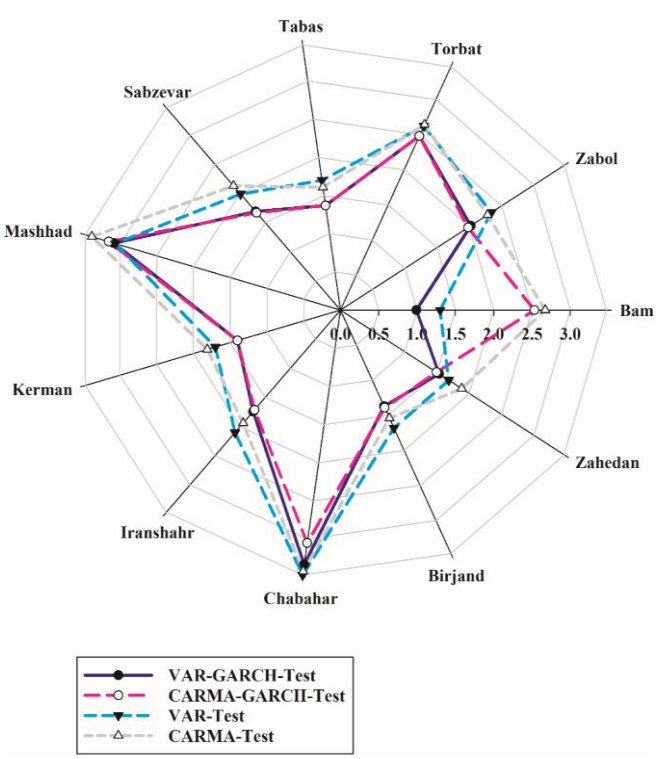

Figure 6. Model error measure (RMSE) of the stations in the testing phase

Taylor and Violin diagram

Figure (7) displays the Taylor diagram, while Figure (8) exhibits the violin diagram, which represents the similarity of time series for the Bam station. It is evident from Figure (7) that the VAR-GARCH model exhibits higher certainty and correlation compared to the other models. On the other hand, Figure (8) reveals that the VAR-GARCH model successfully simulates the quartiles of the data, but it struggles in predicting the minimum and maximum dew point temperatures. In fact, none of the four models examined in this station were able to accurately predict the minimum and maximum data values.

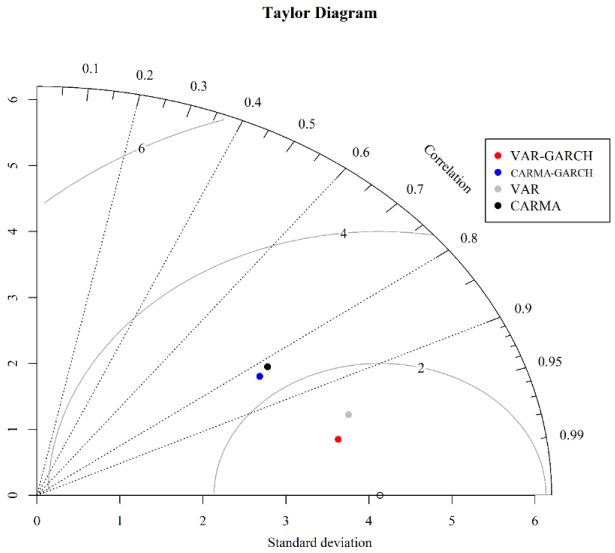

Figure 7. Taylor diagram of Bam station in the test phase

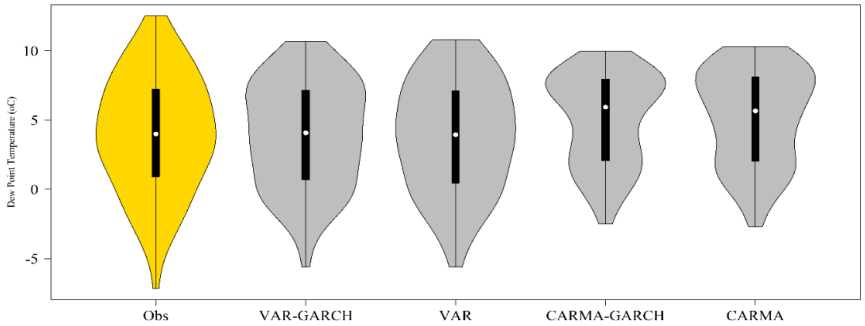

Figure 8. Violin diagram (similarity of time series) of BAM station in the testing phase

The Taylor and Willin diagram was also examined for other stations. After validating four different models, it was found that the VAR-GARCH model had the least amount of error at the Bam station, with an error rate of 0.99 degrees Celsius. The VAR model ranked second at this station, with an error rate of 1.3 degrees Celsius for dew point estimation. This error rate is approximately 31% higher than the value calculated by the first model.

On the other hand, the first pattern (CARMA) had the highest amount of errors and was ranked fourth. Overall, based on the RMSE, the VAR-GARCH model is considered the best model, followed by the VAR, CARMA-GARCH, and CARMA models. Furthermore, the efficiency criterion also revealed that the VAR-GARCH and VAR models exhibit the highest efficiency compared to the other two models. The efficiency coefficient (Nash-Sutcliffe) also identified the VAR-GARCH, VAR, CARMA-GARCH, and CARMA models as better models, along with RMSE. Meanwhile, the efficiency coefficient of the CARMA and CARMA-GARCH models had lower values.

Conclusion

The dew point values across various climates in Iran were estimated using meteorological data from eleven stations, all classified as dry according to the De Martonne index. The input data for estimating dew point values included maximum, minimum, and average temperatures from 1983 to 2021, which showed the highest correlation with dew point. The estimation was performed using multivariable and nonlinear regression with a support vector approach. Initially, the CARMA and VAR methods were applied. Subsequently, the residual series were

modeled using the ARCH approach, resulting in the development of the CARMA-GARCH and VAR-GARCH models.

The accuracy of the estimates at each step was assessed using RMSE and the Nash-Sutcliffe efficiency (NSE) criterion. The evaluation of the VAR and CARMA models showed that the VAR model outperformed the CARMA model in both training and testing phases, likely due to the VAR model's ability to capture nonlinear components. Furthermore, both the VAR-GARCH and CARMA-GARCH models demonstrated superior performance compared to the base models, as the modeling of the residuals improved the results.

During the testing phase, both VAR-GARCH and CARMA-GARCH models performed similarly; however, the VAR-GARCH model showed a marked advantage over the CARMA-GARCH model in the training phase. The VAR-GARCH model achieved the lowest error rate and the highest model efficiency for Bam station, with an RMSE of 0.99°C and a Nash-Sutcliffe coefficient of 0.94, representing the best performance among all stations and models tested.

The number of input parameters for the three-variable model depends on the temperature type. Generally, a model that produces accurate results with fewer inputs is more efficient than one requiring many parameters. Based on these findings, the investigations indicate that the VAR-GARCH model exhibited superior performance during the training phase and demonstrated lower error rates and higher efficiency across most stations. Thus, the VAR-GARCH model can be considered the best model examined in this research.

Statements and Declarations

We hereby declare that there are no conflicts of interest related to this publication and that no substantial financial backing was received that could have biased the results. We further affirm that the manuscript has been thoroughly reviewed and endorsed by all listed authors and that there are no additional individuals who meet the authorship criteria but are not credited as authors. We additionally verify that the sequence of authors presented in the manuscript has been unanimously agreed upon by all co-authors.

Funding

The authors declare that they did not receive any financial backing or sponsorship from any organizsation for the work presented in this submission.

Competing Interests

The authors declare that they have no pertinent financial or non-financial conflicts of interests to report.

Author Contributions

Every contributer played a role in the development of the research's concept and methodology. The preparation of materials, data acquisition and analysis were carried out by Vahid Khorram Nezhad, Abolfazl Akbarpour and M Nazeri Tahroudi. The first draft of the manuscript was written by Vahid Khorram Nezhad and every contributor provided feedback on earlier drafts of the manuscript. Additionally, All contributors thoroughly reviewed and endorsed the ultimate submission..”

Data availability

The underlying data for this study can be obtained by contacting the corresponding author.

References

Aguirre-Gutiérrez, C. A., Holwerda, F., Goldsmith, G. R., Delgado, J., Yepez, E., Carbajal, N., and Arredondo, J. T. 2019. The importance of dew in the water balance of a continental semiarid grassland. Journal of Arid Environments. 168, 26-35.

Baguskas, S. A., King, J. Y., Fischer, D. T., D’Antonio, C. M., and Still, C. J. 2016. Impact of fog drip versus fog immersion on the physiology of Bishop pine saplings. Functional Plant Biology. 44(3), 339-350.

Campbell, J. Y., Lo, A. W., MacKinlay, A. C., and Whitelaw, R. F. 1998. The econometrics of financial markets. Macroeconomic Dynamics. 2(4), 559-562.

Cuthbertson, K., and Nitzsche, D. 2005. Quantitative financial economics: Stocks, bonds and foreign exchange. John Wiley and Sons.

Engle, R. 1982. Autoregressive conditional heteroscedasticity with estimates of the variance of United Kingdom inflation. Econometrica. 50, 391-407.

Hamilton, J. D. 2020. Time series analysis. Princeton University Press.

Lin, J., Shahzad, M. W., Li, J., Long, J., Li, C., and Chua, K. J. 2021. A robust physics-based model framework of the dew point evaporative cooler: From fundamentals to applications. Energy Conversion and Management. 233, 113925.

Lütkepohl, H. 1991. Introduction to multiple time series. Berlin: Springer-Verlag.

Lütkepohl, H. 2001. Vector autoregressions. In Companion to Theoretical Econometrics (pp. 678-699). Blackwell, Oxford.

Maestre-Valero, J., Martin-Gorriz, B., and Martínez-Alvarez, V. 2015. Dew condensation on different natural and artificial passive surfaces in a semiarid climate. Journal of Arid Environments. 116, 63-70.

Mills, T. C., and Markellos, R. N. 2008. The econometric modelling of financial time series. Cambridge University Press.

Ramezani, Y., Nazeri Tahroudi, M., De Michele, C., and Mirabbasi, R. 2023. Application of copula-based and ARCH-based models in storm prediction. Theoretical and Applied Climatology. 151(3), 1239-1255.

Shahidi, A., Ramezani, Y., Nazeri-Tahroudi, M., and Mohammadi, S. 2020. Application of vector autoregressive models to estimate pan evaporation values at the Salt Lake Basin, Iran. IDŐJÁRÁS/Quarterly Journal of the Hungarian Meteorological Service. 124(4), 463-482.

Sims, C. A. 1980. Macroeconomics and reality. Econometrica: Journal of the Econometric Society. 1-48.

Tomaszkiewicz, M., Abou Najm, M., Zurayk, R., and El-Fadel, M. 2017. Dew as an adaptation measure to meet water demand in agriculture and reforestation. Agricultural and Forest Meteorology. 232, 411-421.

Tsay, R. S. 2005. Analysis of financial time series. John Wiley & Sons.

Waggoner, D. F., and Zha, T. 1999. Conditional forecasts in dynamic multivariate models. Review of Economics and Statistics. 81(4), 639-651.

Watson, M. W. 1994. Vector autoregressions and cointegration. In Handbook of Econometrics (pp. 2843-2915).

Yokoyama, G., Yasutake, D., Minami, K., Kimura, K., Marui, A., Yueru, W., and Kitano, M. 2021. Evaluation of the physiological significance of leaf wetting by dew as a supplemental water resource in semi-arid crop production. Agricultural Water Management. 255, 106964.

Zhang, Q., Wang, S., Yang, F.-L., Yue, P., Yao, T., and Wang, W.-Y. 2015. Characteristics of dew formation and distribution, and its contribution to the surface water budget in a semi-arid region in China. Boundary-Layer Meteorology. 154, 317-331.

Zhang, Q., Wang, S., Yue, P., and Wang, S. 2019. Variation characteristics of non-rainfall water and its contribution to crop water requirements in China's summer monsoon transition zone. Journal of Hydrology. 578, 124039.

Appendix

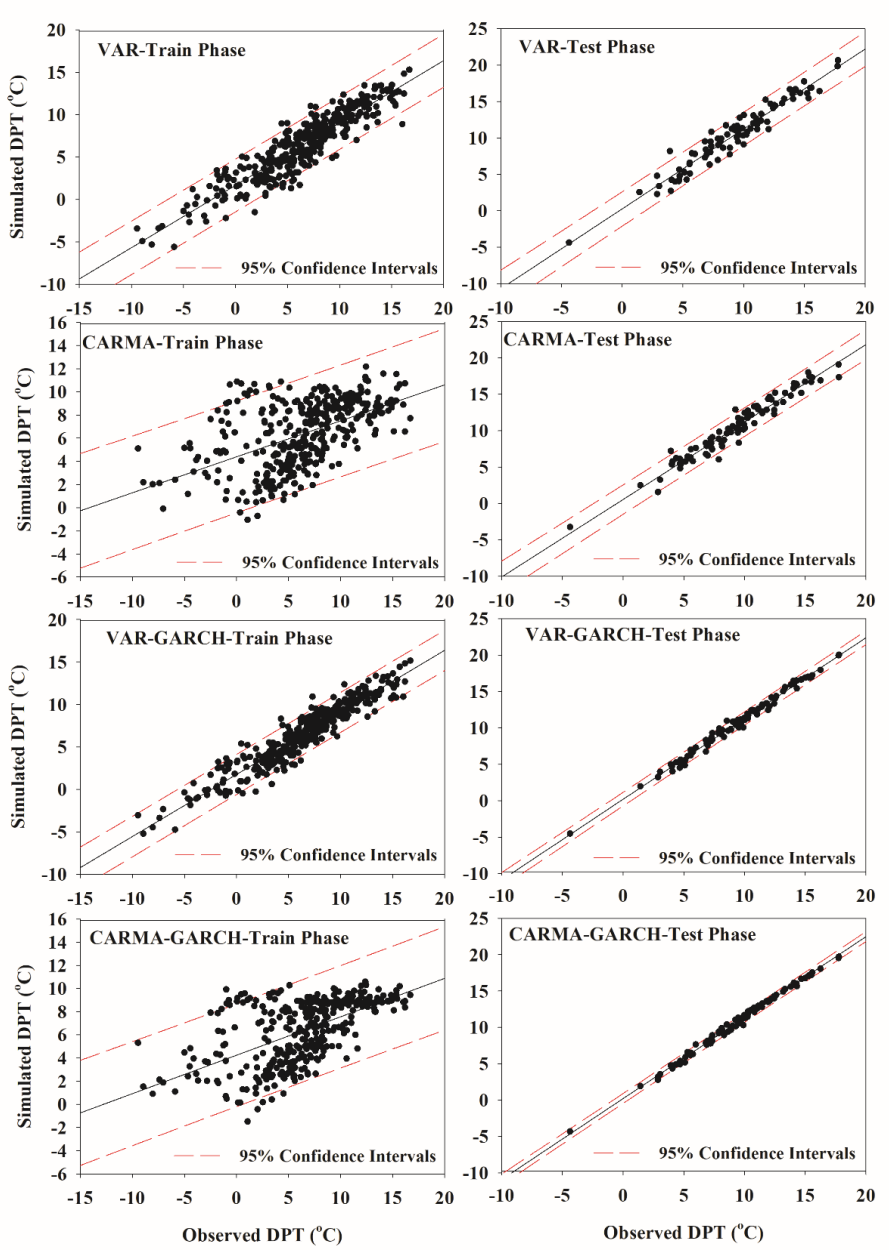

Figure A.1. The results of checking and measuring the accuracy of estimated dew point values in Birjand station

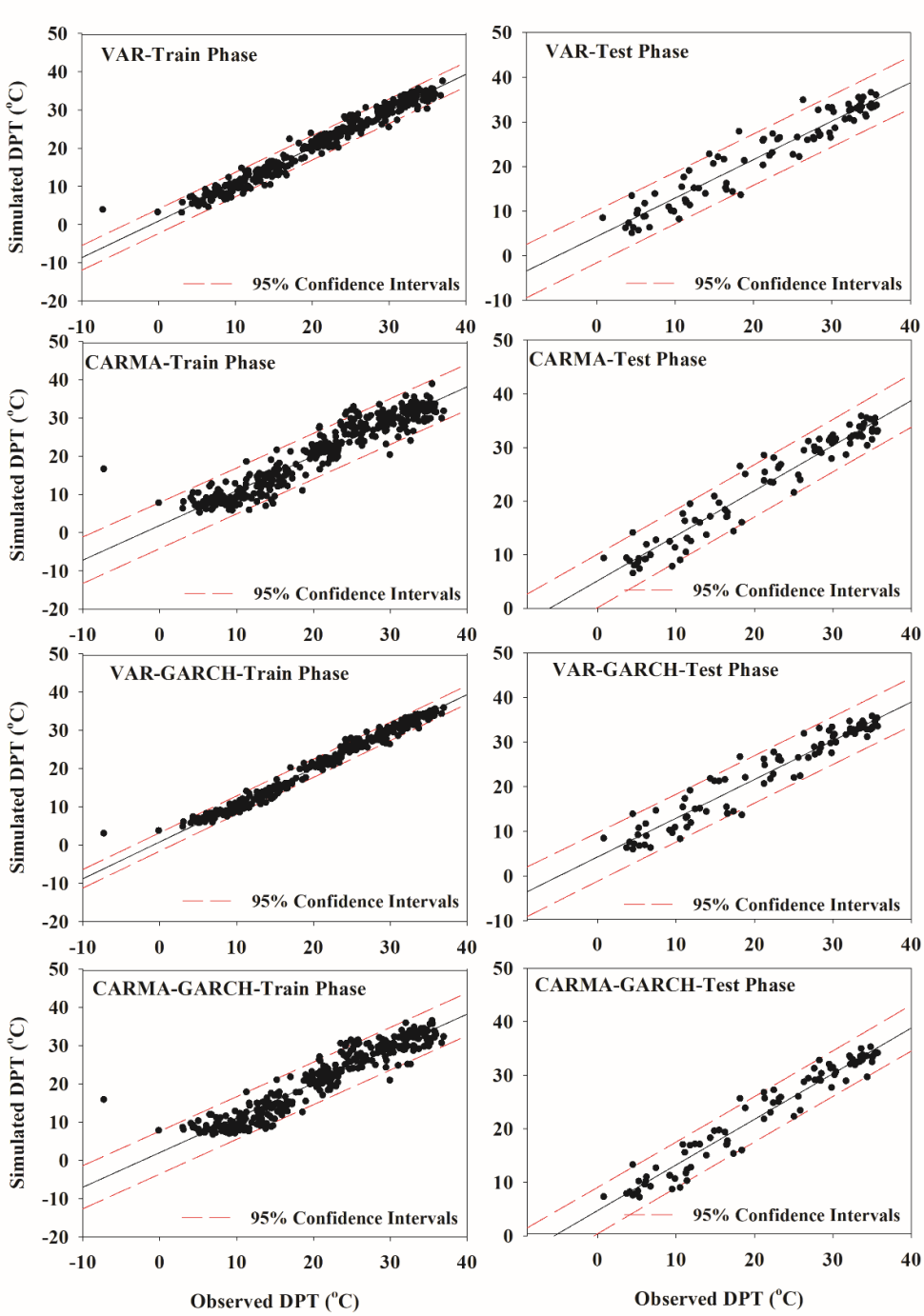

Figure A. 2. The results of checking and measuring the accuracy of estimated dew point values at Chabahar station

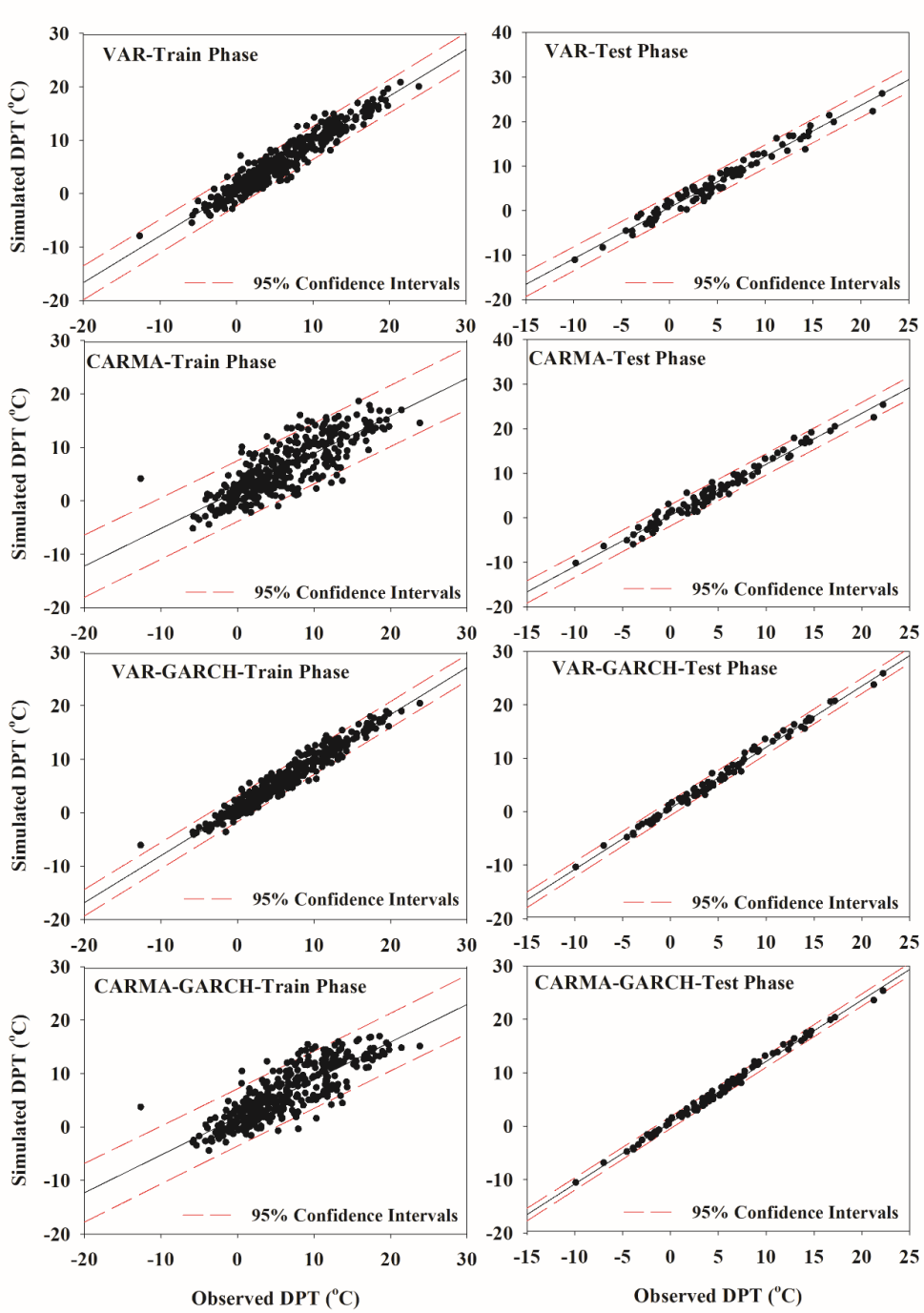

Figure A. 3. The results of checking and measuring the accuracy of estimated dew point values at Iranshahr station

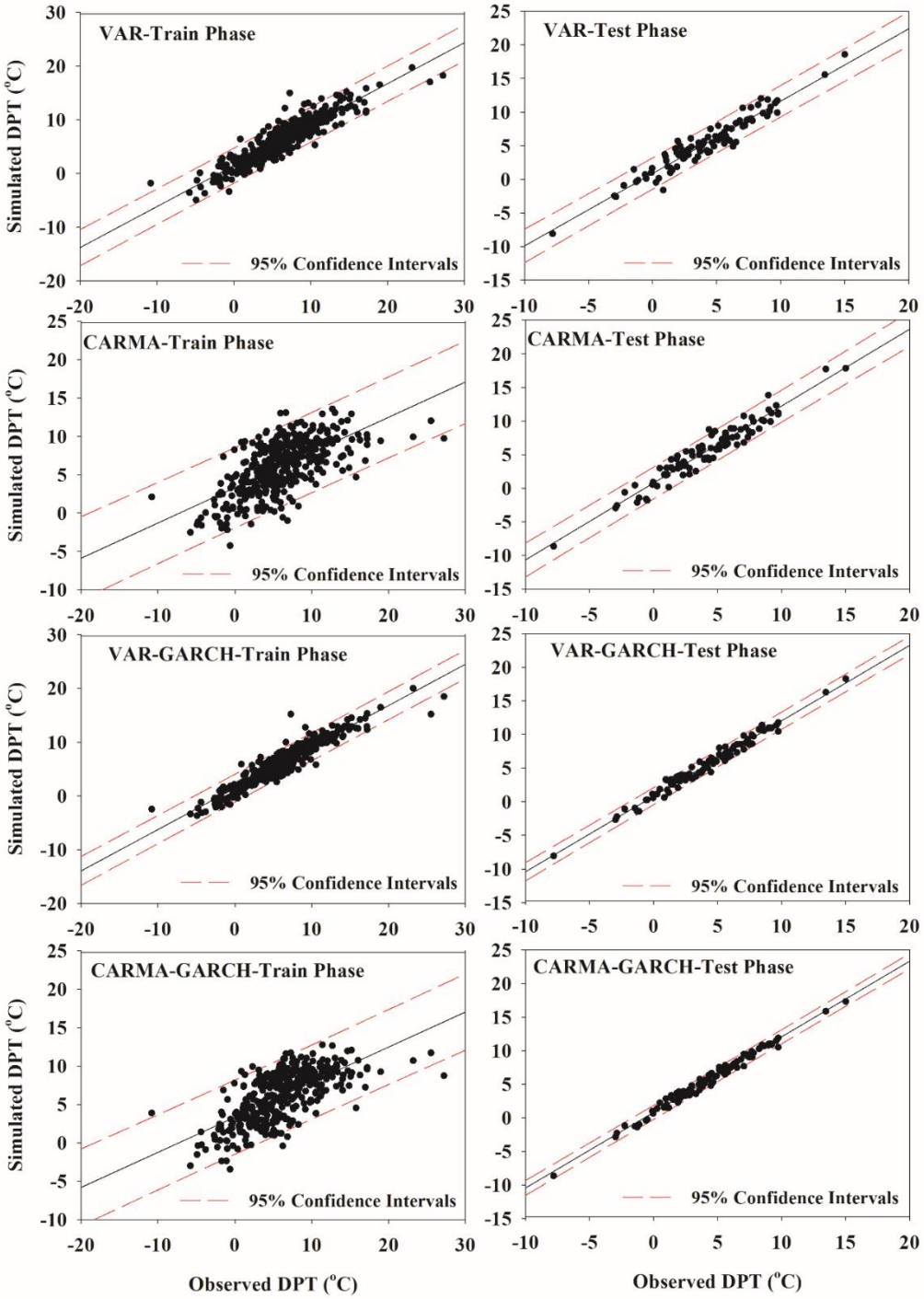

Figure A. 4. The results of checking and measuring the accuracy of estimated dew point values in Kerman station

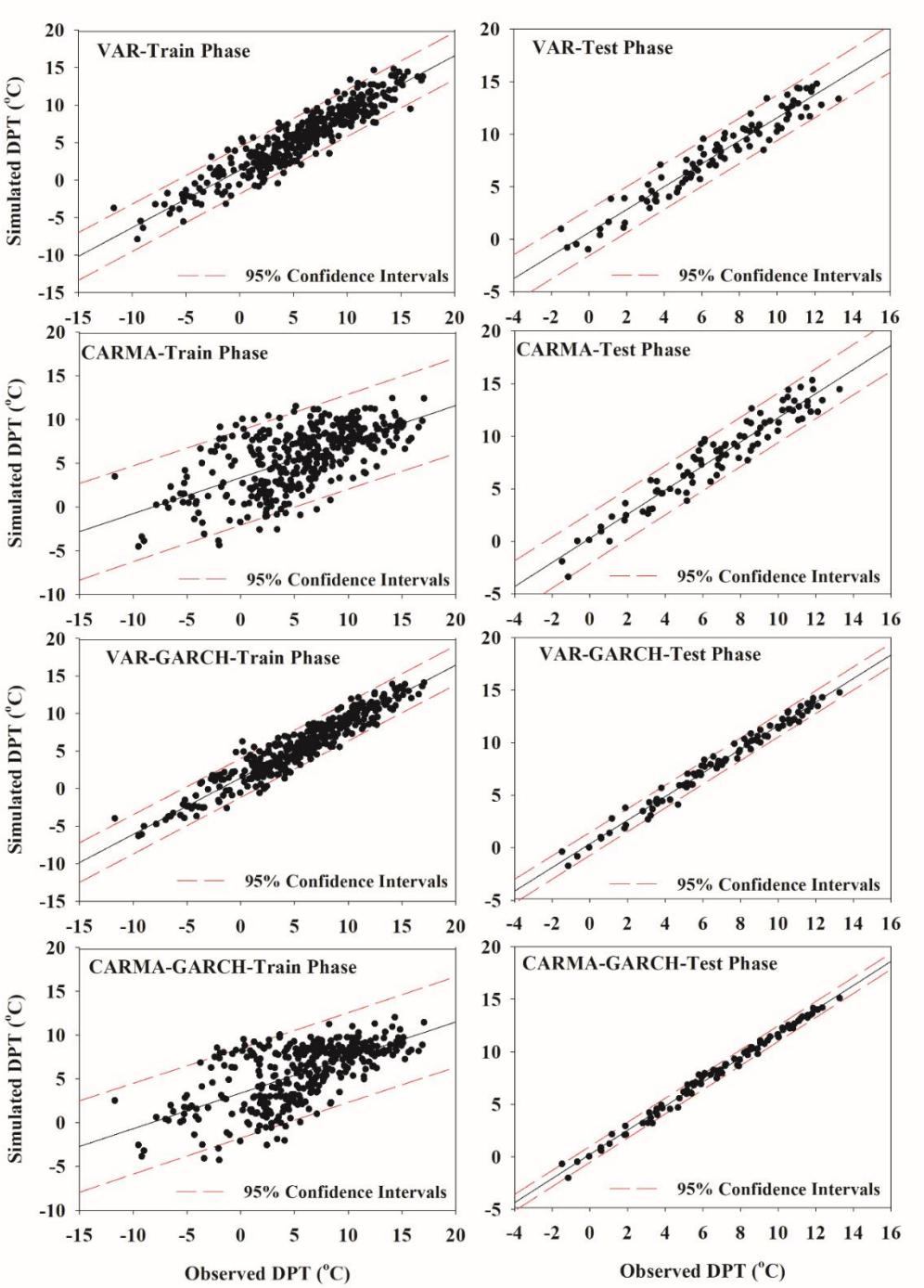

Figure A. 5. The results of checking and measuring the accuracy of estimated dew point values in Mashhad station

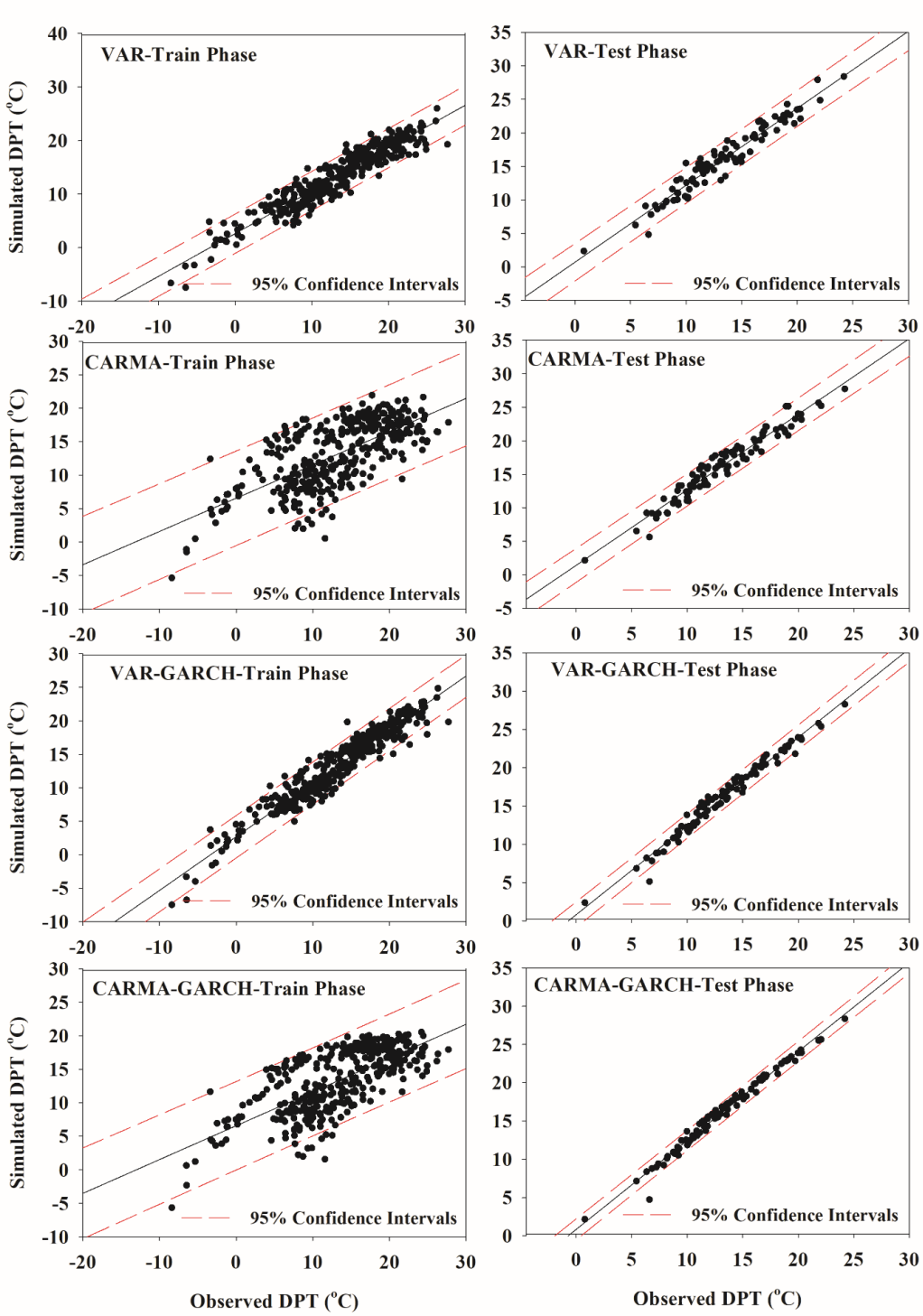

Figure A. 6. The results of checking and measuring the accuracy of estimated dew point values at Sabzevar station

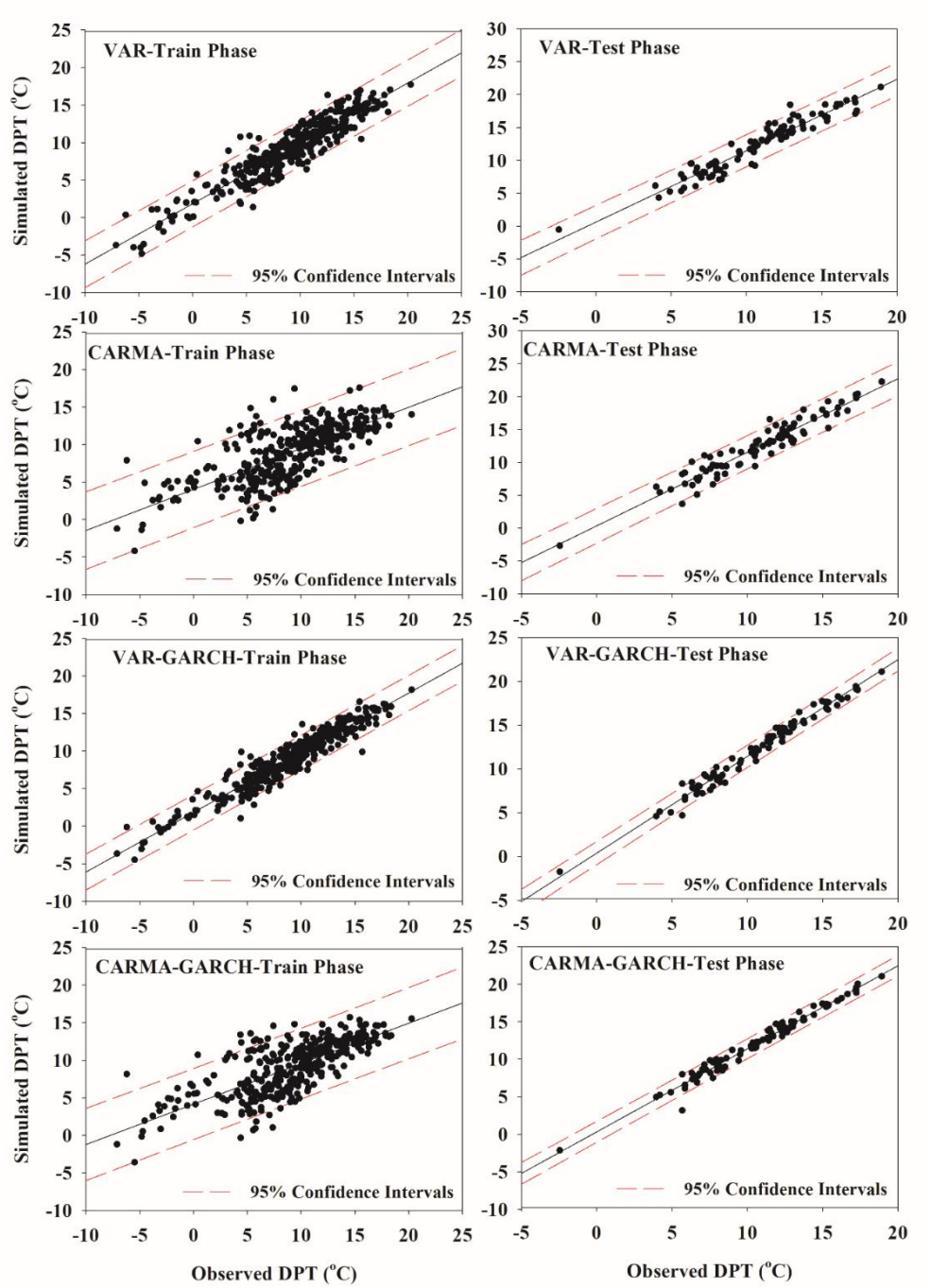

Figure A. 7. The results of checking and measuring the accuracy of estimated dew point values at Tabas station

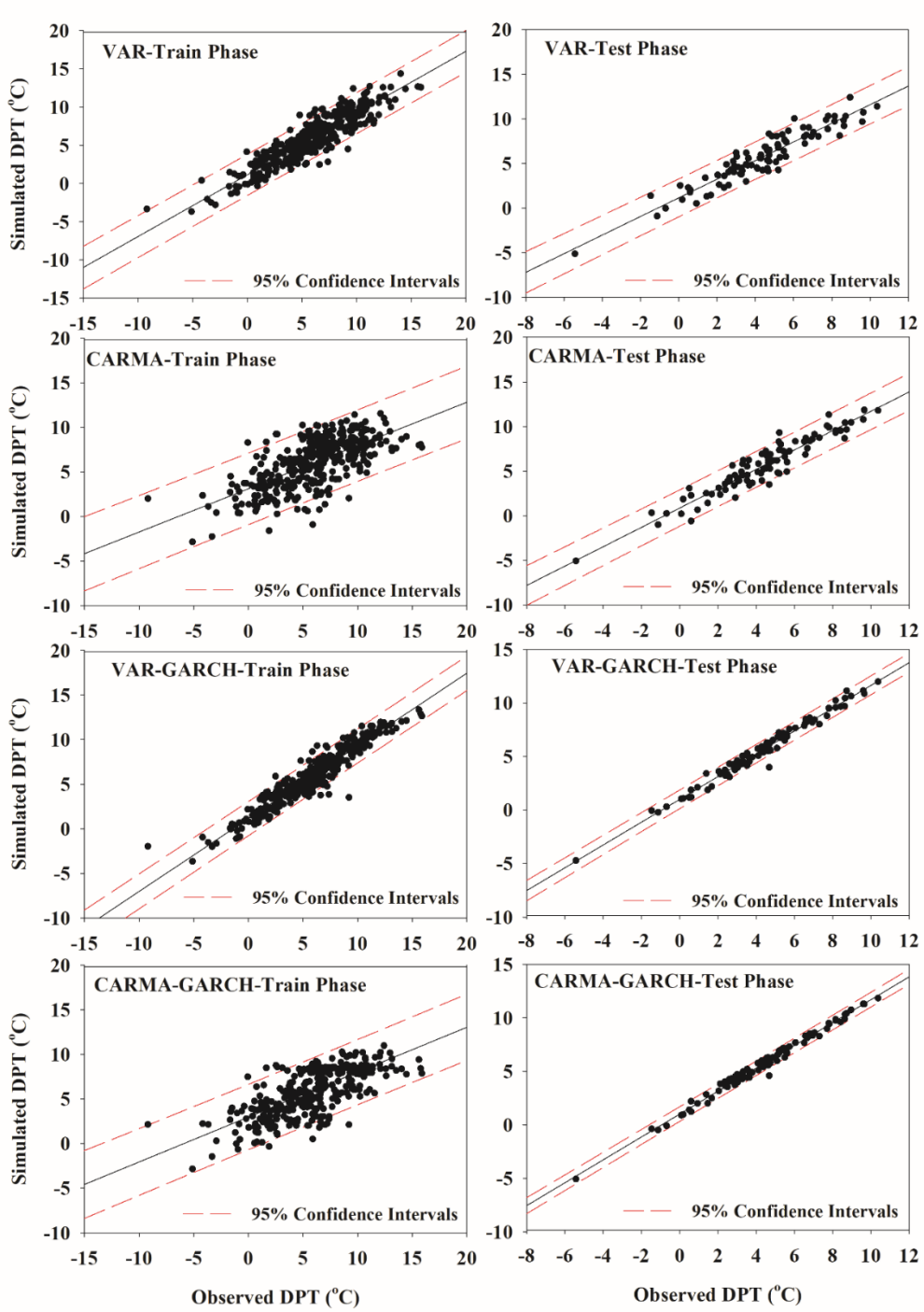

Figure A. 8. The results of checking and measuring the accuracy of estimated dew point values at Torbat Heydarieh station

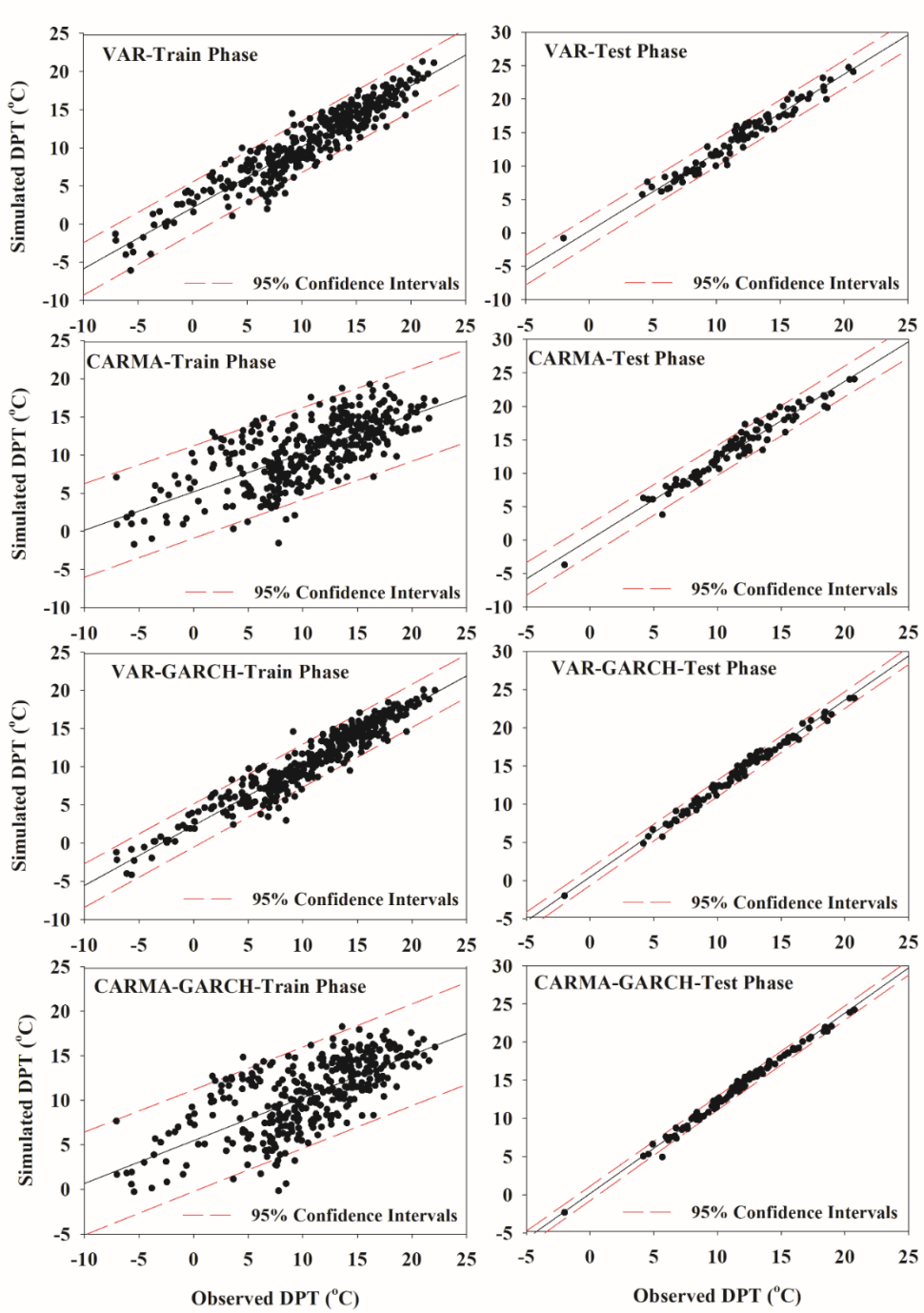

Figure A. 9. The results of checking and measuring the accuracy of estimated dew point values at Zabol station

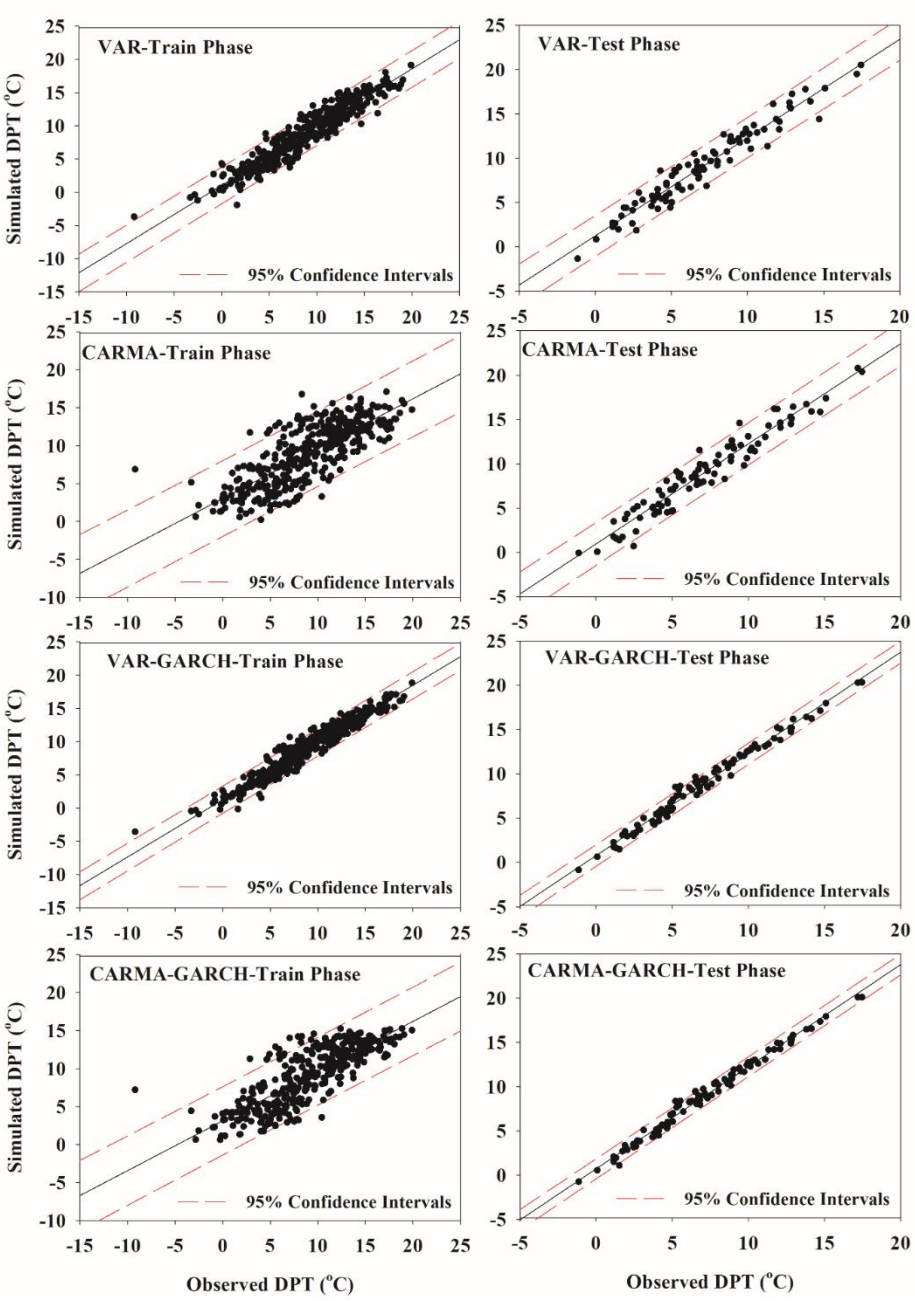

Figure A. 10. The results of checking and measuring the accuracy of estimated dew point values at Zahedan station